Multimodal optical workstation for simultaneous linear, nonlinear microscopy and nanomanipulation: Upgrading a commercial confocal inverted microscope

Manoj Mathew,[a] Susana I. C. O. Santos, Dobryna Zalvidea, and Pablo Loza-Alvarez
ICFO-Institut de Ciències Fotòniques, Mediterranean Technology Park, 08860 Castelldefels, Barcelona, Spain

(Received 24 November 2008; accepted 28 April 2009; published online 1 July 2009)

In this work we propose and build a multimodal optical workstation that extends a commercially available confocal microscope (Nikon Confocal C1-Si) to include nonlinear/multiphoton microscopy and optical manipulation/stimulation tools such as nanosurgery. The setup allows both subsystems (confocal and nonlinear) to work independently and simultaneously. The workstation enables, for instance, nanosurgery along with simultaneous confocal and brightfield imaging. The nonlinear microscopy capabilities are added around the commercial confocal microscope by exploiting all the flexibility offered by this microscope and without need for any mechanical or electronic modification of the confocal microscope systems. As an example, the standard differential interference contrast condenser and diascopic detector in the confocal microscope are readily used as a forward detection mount for second harmonic generation imaging. The various capabilities of this workstation, as applied directly to biology, are demonstrated using the model organism *Caenorhabditis elegans*. © *2009 American Institute of Physics.* [DOI: 10.1063/1.3142225]

I. INTRODUCTION

Ever since its introduction, the confocal microscope[1–3] has emerged as a very powerful and indispensable tool for biological imaging. Its ability to provide excellent axial resolution, collect three-dimensional images of thick fluorescently labeled specimens, together with the user friendliness and versatility of modern day commercial confocal microscopes, has made it the biologist's preferred imaging tool.

Linear fluorescence microscopy, which forms the basis of confocal fluorescence microscopy, however, suffers from fundamental penalties (such as enhanced photodamge and low depth of penetration among many others) owing to the use of shorter wavelengths for excitation. Nonlinear/multiphoton microscopy techniques such as two-photon excited fluorescence (TPEF) microscopy[4] aim to overcome these problems partly by the use of near-infrared (NIR) light for excitation. Harmonic generation microscopy [second harmonic generation[5] (SHG) and third harmonic generation[6,7] (THG) microscopy] goes a step further by providing intrinsic contrast (without the need for labeling and thus not causing photobleaching) and structural information below the resolution limit of light.[8] Moreover, a nonlinear microscope can be used to perform nanomanipulation techniques such as nanosurgery.[9,10] Hence, nonlinear microscopes provide immense possibilities in biological investigation.

A tool that would allow full use of the advantages of both a multiphoton and a commercial confocal microscope, in such a way that both systems could work simultaneously, is, however, lacking. Such a tool would allow the simultaneous gathering of information about active biological processes using different techniques. In biology, such gathering of as much information as possible about a biological process using numerous techniques in a given instant of time is of fundamental importance. For instance, it is particularly valuable to image the site of nanosurgery in real time using multiple techniques (e.g., brightfield and confocal microscopy). This not only aids the selection of target structures, but also provides a wealth of information about the temporal evolution of structural changes induced by the procedure. This, however, requires a device that has two independent optical systems that direct two sets of laser beams simultaneously and independently (one to induce an effect and the other to perform optical imaging). A tool with simultaneous capabilities of a commercial confocal microscope and multiphoton microscope would be, therefore, a great asset in such cases where simultaneous imaging and manipulation is required. Another interesting possibility of such a system is multimodal imaging combining linear and nonlinear techniques. This could be interesting, for instance, in cases where a particular structure could be imaged with SHG and structures around it, labeled with multicolored fluorophores, could be simultaneously imaged with multispectral confocal fluorescence microscopy.

In this work we build, for the first time to our knowledge, a nonlinear/multiphoton microscope having a commercial confocal microscope as base (inverted Nikon C1-Si) in a way that both the confocal and multiphoton sections can work independently and simultaneously. This is done without tampering with any of the confocal microscope system (such as the scan and detection heads). We fully exploit all the flexibility, offered by the commercial confocal system [such as two filter turrets, four detection ports, differential interference contrast (DIC) condenser, and diascopic detector] and

[a]Electronic mail: manoj.mathew@icfo.es.

add: (1) a separate scan head (SH), (2) separate detection systems, both in the forward and backward directions, and (3) separate control systems and software. All these features are achieved without the need to alter any of the C1-Si microscope components.

Modern day commercial confocal microscopes combine DIC microscopy, epifluorescence microscopy, multichannel confocal microscopy, laser-scanning brightfield (LSBF) microcopy by diascopic detection of scanned laser (confocal excitation) beam, and, recently, even spectrally resolved confocal microscopy. All the above, together with fully automated components, software control, and image processing /analysis tools[11] make commercial confocal microscopes very user friendly and versatile devices. The Nikon Confocal C1-Si microscope used in this work has all the aforementioned features. In addition to these features we have added the following tools:

(a) TPEF microscopy.
(b) SHG/polarization sensitive SHG (PSSHG) microscopy.
(c) Femtosecond laser induced stimulation/manipulation.
(d) LSBF microscopy by detection of scanned NIR laser beam (for nonlinear excitation).

All the above mentioned features give the workstation the following capabilities:

(1) Simultaneous LSBF, SHG, and TPEF imaging.
(2) Simultaneous confocal, LSBF, and SHG imaging.
(3) Simultaneous epifluorescence, LSBF, and SHG imaging.
(4) Simultaneous confocal imaging, brightfield imaging, and femtosecond laser induced stimulation/manipulation.
(5) Simultaneous epifluorescence imaging and femtosecond laser induced stimulation/manipulation.

The achieved capabilities 1–4 are being demonstrated for the first time in our knowledge. Moreover, it is the first time, in our knowledge, that all the above five capabilities (1–5) are being offered in one single system. For each of the above mentioned capabilities, a set of illustrative results using the model organism nematode *Caenorhabditis elegans* (*C. elegans*) as the subject of study, are provided. In addition, we demonstrate one of the numerous sub features of the laser manipulation abilities: the nanosurgery in neurons of the same model organism. The combination of all the different imaging techniques with the laser manipulation asset provides us with a state-of-the-art tool for the study of real-time processes in biological functions.

II. THE STATE-OF-THE-ART

Multiphoton microscopes are starting to be fully commercialized. The most currently existing systems are homebuilt. Most of these systems have detection capabilities simultaneously in the forward and backward direction, enabling simultaneous SHG\THG and TPEF microscopy. Nevertheless, since these microscopes use a single scanning system, applications such as simultaneous femtosecond laser induced nanosurgery and depth resolved imaging are not feasible.

Since multiphoton and confocal microscopes share a very similar scanning and detection platform, a number of attempts have been made to convert commercial confocal systems into tools for nonlinear microscopy. This enables ease of fabrication, user friendliness, and, most importantly, takes the nonlinear microscope much closer to the targeted end user: the biologists who are very familiar with the use of confocal microscopes. Most of these works[12–16] have attempted to route the ultrashort NIR light for nonlinear microscopy through the confocal SH. This allows easy control of the microscope by a novice user (by using the confocal microscope controls and software). This configuration has, however, two distinct drawbacks: (1) the confocal scan and detection heads have to be opened and modified to enable it to switch between confocal and multiphoton modes and (2) the microscope can, at a time, work either as a confocal microscope or as a nonlinear microscope, but not both simultaneously.

Commercial multiphoton microscopes that have two separate systems to direct two laser beams simultaneously (in a way that one laser is used for stimulation and the other for imaging) do exist.[17,18] However, such systems rely on dedicated intricate optomechanical setups incorporated to the microscope and, to the best of our knowledge, they do not provide the ability to perform linear and nonlinear imaging (using the two scanning systems together) simultaneously.

There have also been attempts by research groups to set two independent laser-scanning systems together to allow, for example, the ability to combine optical tweezing with multiphoton microscopy.[19] Other groups have worked on developing multimodal imaging systems in which combined multiphoton techniques, such as coherent anti-Stokes Raman scattering, sum-frequency generation imaging, and TPEF, have been demonstrated by making use of two synchronized laser-scanning systems.[20]

III. MATERIALS AND METHODS

A. Construction of the microscope

The construction of the multimodal workstation is described in this section in detail and it follows the actual sequence of the workstation construction. Starting from the femtosecond laser, (a) steering the laser beam onto the galvanometric mirrors, (b) describing the confocal microscope, (c) steering the light inside the microscope, and d) implementation of the forward detection system. The description ends with (e) a small account of the signal acquisition system, control, and software used.

1. Steering the femtosecond light onto the galvanometric mirrors

The schematic of the setup is shown in Fig. 1. The femtosecond laser (to be used for nonlinear applications) is brought into the workstation (in the biolab) from an adjacent room. The laser used is a Kerr lens mode locked Ti:sapphire laser (Coherent MIRA 900 f), which can operate both in femtosecond (160 fs pulse duration, pulse repetition rate of 76 MHz) and continuous wave (CW) regimes with wavelength tunable from 650 to 900 nm.

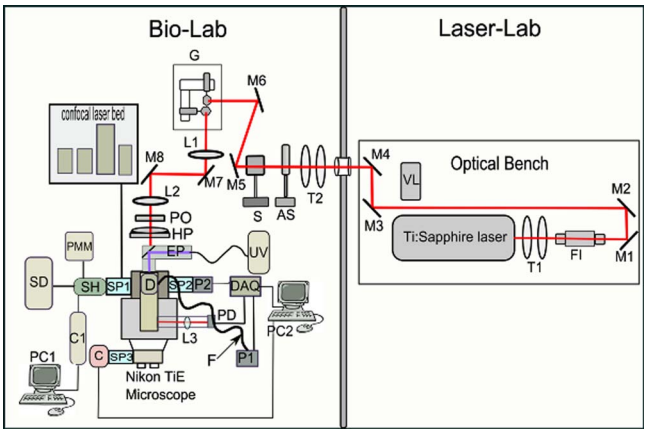

FIG. 1. (Color online) Schematic diagram of the setup developed around the Nikon C1-Si confocal microscope. The setup is composed of two optical benches: one inside the laser laboratory and other in inside the biology laboratory. T-telescope, M-mirror, VL-Verdi laser, FI-Faraday isolator, AS-attenuator set, S-electronic shutter, G-galvanometric mirror, L-lens, PMM-photomultiplier module, SD-spectral detector, SH-scan head, C1-confocal microscope control box, C-CCD camera, SP-side port, D-diascopic port, F-optical fiber, PO-linear polarizer, HP-half wave plate, P-photomultiplier tube, EP-epifluorescence attachment, DAQ-data acquisition system, PD-photodiode, UV-xenon lamp, and PC-computer, confocal laser bed with a set of four lasers (two diode lasers, one He–Ne laser and one argon ion laser).

The femtosecond light beam from the laser passes through a telescope (T1) (expands to approximately 5 mm in diameter) and a Faraday isolator (FI) to avoid any back reflections from destabilizing the laser mode lock operation. The telescope is used to reduce the beam intensity to a value below the damage threshold of the FI as well as to compensate, to some extent, the large beam divergence caused by the significant distance between the femtosecond laser and the microscope.

Once in the biolab the beam passes through an attenuator set (AS) composed by two attenuators (attenuator 1 and attenuator 2), and an electronically controlled shutter (S). The attenuators are placed side by side on a motorized translation stage [Physik Instrumente (PI), M-505]. This enables the selection of two different optical powers under computer control, depending on which attenuator is placed in the beam path. This configuration is useful, for instance, when quickly changing from imaging mode to nanosurgery mode (where imaging power is significantly different from the nanosurgery power). In order to reduce expense, a homemade shutter was built using a blackened metal plate mounted on an audio speaker. By applying the correct voltage (under computer control) the speaker membrane moves up/down, shifting the metal plate in and out of the beam. The shutter is able to switch between states in less than 100 ms.

Using a set of mirrors the beam is subsequently steered onto the galvanometric system (G) (Cambridge Technology 6215 H). To reduce loss in the 3 mm galvanometric mirrors the beam is reduced to half its size (2.5 mm) using a telescope (T2) before the attenuator. The light after the galvanometric system passes through a third telescope with lenses L1 and L2, and is directed into the workstation. L1 and L2 serve two functions: (1) to image the galvanometric mirrors onto the back aperture of the objective, and (2) to expand the beam five times (to about 12.5 mm) to overfill the back aperture (10 mm) of the 60× high numerical aperture (NA) (1.4 NA) objective (details of multiphoton microscope design can be found in Ref. 21). To aid PSSHG imaging a linear polarizer (LP) and a half wave plate (HP) mounted on graduated rotating stage are placed after L2. Although the light coming out of the Ti:sapphire is linearly polarized, there can be some degree of depolarization arising out of the numerous optics in the beam path. A LP was therefore added and rotated to provide maximum transmission. The angle of polarization of the incident femtosecond light could then be changed accurately by rotating the graduated HP.

2. The confocal microscope

A Nikon C1-Si (Nikon Inc., Japan) confocal laser-scanning imaging system[11] built onto a Nikon inverted research microscope T*i*-E is employed in the setup. The C1-Si system offers standard three channel detection as well as spectrally resolved detection modes. In addition to standard DIC microscopy, it offers LSBF imaging (by diascopic detection of forward scattered excitation laser light during confocal laser scanning) simultaneously with confocal imaging.

The diascopic detector consists of an optical fiber with one of its ends mounted inside the microscope illumination tower, between the collector lens and the lamp. The collector lens focuses the forward scattered excitation light. This light is reflected by a mirror mounted on a slider and is focused onto the fiber tip. The mirror when slid out enables the illumination light form the lamp to pass onto the collector lens to enable conventional brightfield imaging. The other end of the fiber is inserted into the confocal microscope C1 control box where a silicon photodiode (PD) detects the forward scattered light.

The excitation for confocal microscopy is provided by a set of four lasers (two diode lasers, one He–Ne laser, and one argon ion laser) mounted on a laser bed. This allows seven excitation wavelengths (405, 457, 477, 488, 514, 561, and 635 nm) to be used simultaneously. Light from the laser sources are combined in the laser bed and brought into the SH using an optical fiber cable. The SH is attached to the side port (side port 1) of the microscope (Fig. 1). The emission light resulting from confocal laser scanning is descanned by the SH and delivered to the regular three channel detector module [photomultiplier module (PMM)] or the spectral detector (SD), both of which are connected to the SH (using optical fiber cables). The confocal microscope systems are controlled by the C1 controller along with the computer (PC1).

The Nikon Eclipse T*i*-E (Ref. 22) (Nikon Inc., Japan) used in the setup is a fully motorized advanced research microscope which provides DIC imaging using a DIC condenser and halogen lamp as well as epifluorescence imaging using an epifluorescent attachment (EP) and UV lamp. The microscope provides two back ports (back port 1 and back port 2) and four side ports (side ports 1–4) (see Figs. 1 and 2 for details). The two back ports are positioned on top of each other. The microscope uses two motorized filter turrets where filter turret B is mounted on top of filter turret A (see Fig. 2 for details). Excitation light transmitted in the forward direction is collected by the DIC condenser and can be directed

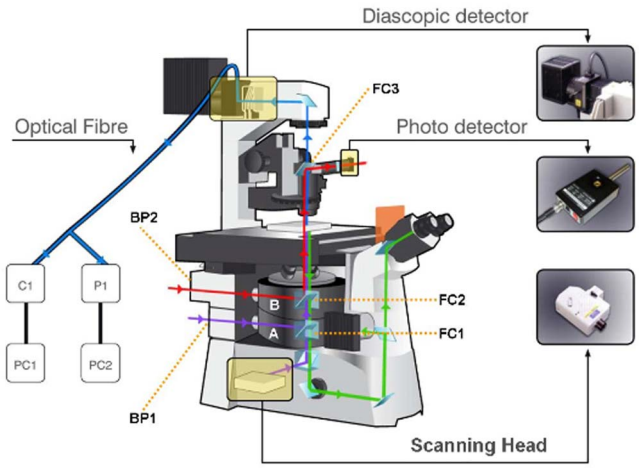

FIG. 2. (Color online) An artist's impression of the multimodal microscope system with its various light paths. Green light path-backward detected fluorescence, violet light path-epifluorescene and confocal excitation, blue light path-forward propagating SHG signal, red light path-NIR excitation, PC-computer, C1-confocal microscope control box, P1-PMT module 1, A-filter turret A, B-filter turret B, BP-back port, and FC-filter cube.

into the optical fiber which forms part of the diascopic detector to generate the LSBF simultaneously with confocal imaging.

3. Steering the light inside the microscope

The EP for epifluorescence microscopy is mounted on the first back port (back port 1) and the corresponding filter cubes (FC1a–FC1c) are mounted in filter turret A (Fig. 2). The filter turret employs standard filter sets for green fluorescent protein (GFP), yellow fluorescent protein (YFP), and DsRed mounted in filter cubes FC1a, FC1b, and FC1c, respectively. The femtosecond laser light is directed through the second back port (back port 2) into the filter turret B with a filter cube FC2. A dichroic mirror in FC2 (Semrock, Inc., FF670-SDi01, *T*: 360–650 nm, *R*: 680–1080 nm) is used to reflect the femtosecond laser beam up toward the objective. This dichroic mirror allows the fluorescence excitation from below and fluorescence emission light from the sample plane to pass through it. In the epifluorescence mode, FC1 is inserted, while in confocal microscopy mode, no filter cube is used in the filter turret A (the confocal microscope does not use the filter sets inside the base microscope; the filtering is done externally). This configuration allows simultaneous interaction of the femtosecond laser light and fluorescent excitation for epifluorescence/confocal microscopy with the sample plane.

A complete illustration of the different light paths that compose this multimodal system can be found in Fig. 2 where violet lines indicate fluorescent excitation light in confocal and epifluorescent modes. Red lines indicate NIR excitation light (directed onto the sample as well as transmitted through the sample onto the photodetector) for nonlinear microscopy, LSBF, and nanosurgery. Blue lines indicate forward propagating SHG signal.

4. Detection in the backward direction

The generated fluorescence from the sample that is collected by the objective lens passes back through the dichroic mirror in FC2 (in filter turret B) (Fig. 2). In epifluorescence microscopy mode this light, after passing through the barrier filter in FC1 (in filter turret A), passes on to a charge coupled device (CCD) camera (Hamamatsu ORCA R2) attached to side port 3. In confocal microscopy mode the backward returning light passes on to the SH in side port 1. In multiphoton mode it passes to side port 2 where a photomultiplier tube (PMT) module (P2) (Hamamatsu, H9305-03) detects the TPEF signal. A band pass filter (Chroma technologies, custom GFP filter) was inserted into the PMT module to filter the fluorescence form GFP-labeled samples. This filter can be easily swapped for others for different fluorescent markers. The ports are changed under computer control depending on the mode of operation.

5. Detection in the forward direction

The standard DIC condenser (0.5 NA front lens) and the diascopic detector are used as a forward detection mount to aid SHG imaging. The optical fiber from the diascopic system is inserted into a second PMT module (P1) (Hamamatsu, H9305-03), which has a removable fiber input mount and an attached narrow band pass filter (Semrock FF01-434/17). The filter is used to transmit only the forward scattered SHG signal. To ensure that all light is collected when a high NA objective lens is used, the 0.5 NA DIC condenser is replaced by a standard oil immersion, high NA DIC condenser [1.4 NA, 1.92 mm working distance (WD), Nikon]. When detecting the SHG signal, the polarizer and DIC prism in either of the DIC condensers are slid out.

The optical fiber cable in the diascopic detector can be readily moved back and forth between the C1 control box (in case of confocal mode of operation) and the PMT module P1 (in multiphoton mode). The diascopic detector enables generation of LSBF images of the sample in confocal mode (by detecting the forward scattered confocal excitation light), while in nonlinear microscopy mode the optical fiber in the diascopic detector enables generation of SHG images.

In order to generate brightfield images in the nonlinear mode a third filter cube (FC3) is placed over the DIC condenser, which contains a second dichroic mirror (Semrock, Inc., FF670-SDi01) that reflects NIR and transmits in visible and UV wavelengths. FC3 is simply placed on top of the slider for the polarizer in the DIC condenser (see Fig. 2). The polarizer is slid out before placing FC3. This enables the unconverted NIR excitation light to be reflected on to a PD (NewFocus, IR photoreceiver 2033) mounted outside the microscope, while directing the rest of the light toward the diascopic detector fiber. A collection lens L3 is used to collect the reflected NIR light and focus onto the photodetector head. Light thus detected forms the third channel in the nonlinear microscopy mode to generate LSBF simultaneously with TPEF and SHG in channels 1 and 2, respectively. The nonlinear mode, hence, provides the capability for simultaneous three channel detection (TPEF, SHG, and LSBF).

6. Signal acquisition, control, and software

The signals from P1, P2, and PD are collected simultaneously using a data acquisition system (DAQ) (National Instruments, PCI-6115) which is controlled using PC2. Hence, the controls of the confocal system are controlled using PC1 and those of the nonlinear microscopy system are controlled using PC2.

An automatized z motion control is used for obtaining image stacks at successive focal planes in the nonlinear mode of operation. This objective axial motion in z is performed in the confocal microscope by a motorized movement controlled by the software in PC1. This control can also be done manually through a dial system provided with the microscope. In order to control the z motion automatically in the multiphoton microscopy mode, a stepper motor (PI, C-136) under the control of PC2 was attached to this manual dial. The distance moved by the objective is read out in micrometers form the microscope digital display.

A homebuilt control software (programmed in LABVIEW 8.5, National Instruments Corporation) is employed for control, image acquisition and storage of images and metadata in the multiphoton microscopy mode. This control software runs in PC2.

B. Microscope sample preparation

For the illustration of the workstation capabilities two different *Caenorhabditis elegans* strains {juIs76 [unc-25::gfp] II and akIs3 (nmr-1::gfp)} expressing GFP in specific neuron types are cultured and grown in large quantities using methods reported previously.[23] A number of healthy worms are mounted on a thin 2% agar pad with an anesthetic between two 40 μm glass slides. The selected anesthetic for immobilization was sodium azide-NaN3 (0.8 μl at 25 mM). The mounts are sealed with melted paraffin wax for stabilization. The worm mounts were only used within a period of less than one hour in order to guarantee the worm physical condition.

C. Characterization of the point spread function

In order to characterize the imaging system we proceed to measure the point spread function (PSF). This was measured for both confocal and two-photon imaging systems, based on Yoo *et al.*[24] and Bigelow *et al.*[25] Submicroscopic G200 polymer microspheres (i.e., 200 nm) were used as point objects. A suspension of 200 nm beads in distilled water was sonicated and placed between two cover glasses and then a focal series of images of single beads was recorded in exactly the same way as for a standard biological sample to obtain the radial PSF at the focal plane. In the axial direction, a z-stack in each configuration was taken. The PSFs were acquired with 60× oil immersion objective, which was used to acquire all images shown in the manuscript.

Using a standard parameter to estimate the size of the image of a point, the full width half at maximum (FWHM) was measured from the plot in the x and z directions.

IV. OPERATIONAL FUNCTIONING AND RESULTS

This section starts by an image quality assessment followed by presenting a detailed description of each of the five capabilities (see introduction section) of the workstation. First a description is provided on how to configure the workstation to enable a particular capability followed by an example illustrating implementation of the capability in a biological sample. Sections IV G and IV H describe special features relating to brightfield imaging and SHG imaging implemented in this workstation.

A. Image quality evaluation

The PSF was measured in the radial and axial directions for both Confocal and nonlinear imaging modalities. The several results are shown in Fig. 3. In order to compare the performance of the different imaging systems, the FWHM was calculated from each cross section of the PSF. For the confocal imaging system, the FWHM in x-direction was around 260 nm [Fig. 3(a)], and in z direction was 1 μm [Fig. 3(b)]. The FWHM for the nonlinear configuration in the x-direction was approximately 400 nm [Fig. 3(c)] and in the z direction was approximately 2 μm [Fig. 3(d)].

B. Simultaneous LSBF, SHG, and TPEF microscopy

In the case of simultaneous LSBF, SHG, and TPEF microscopy, none of the functions of the confocal microscope are required. The filter cube FC2 in filter turret B is placed into the beam path to reflect the NIR femtosecond light (868 nm) onto the objective. The control software in PC2 is used to raster scan the femtosecond laser beam in a region of interest. Emission light in the backward direction is directed into side port 2 to collect the TPEF signal by the PMT (P2). The filter cube FC3 is placed on top of the condenser to reflect the undepleted NIR light onto the PD. The optical fiber cable in the diascopic detector is pulled out form the C1 box and inserted into the PMT module (P1) to detect the SHG signal. The system acquires signals simultaneously from P1, P2, and PD thus enabling simultaneous LSBF, SHG, and TPEF imaging.

The Fig. 4 shows part of an adult *C. elegans* imaged in this modality. In this image, (a) the LSBF image of the whole scanned region can be observed in gray scale, (b) two GFP-labeled *D*-type motor neurons and some autofluorescence from lipofuscin granules can be observed in green color in the TPEF image, (c) and the body wall muscles can be observed in red color in the SHG image. Images in Figs. 4(a)–4(c) were obtained simultaneously form the same scanning process. The figure also depicts a (d) superposition of all the three image channels.

All the above imaging was performed using an average power of 15–18 mW on the sample plane and a wavelength of 868 nm. The wavelength of 868 nm for excitation was chosen to suite the availability of the narrowband pass filter at 434 nm for SHG imaging. This wavelength is also quite suited for exciting GFP as required for the TPEF images.

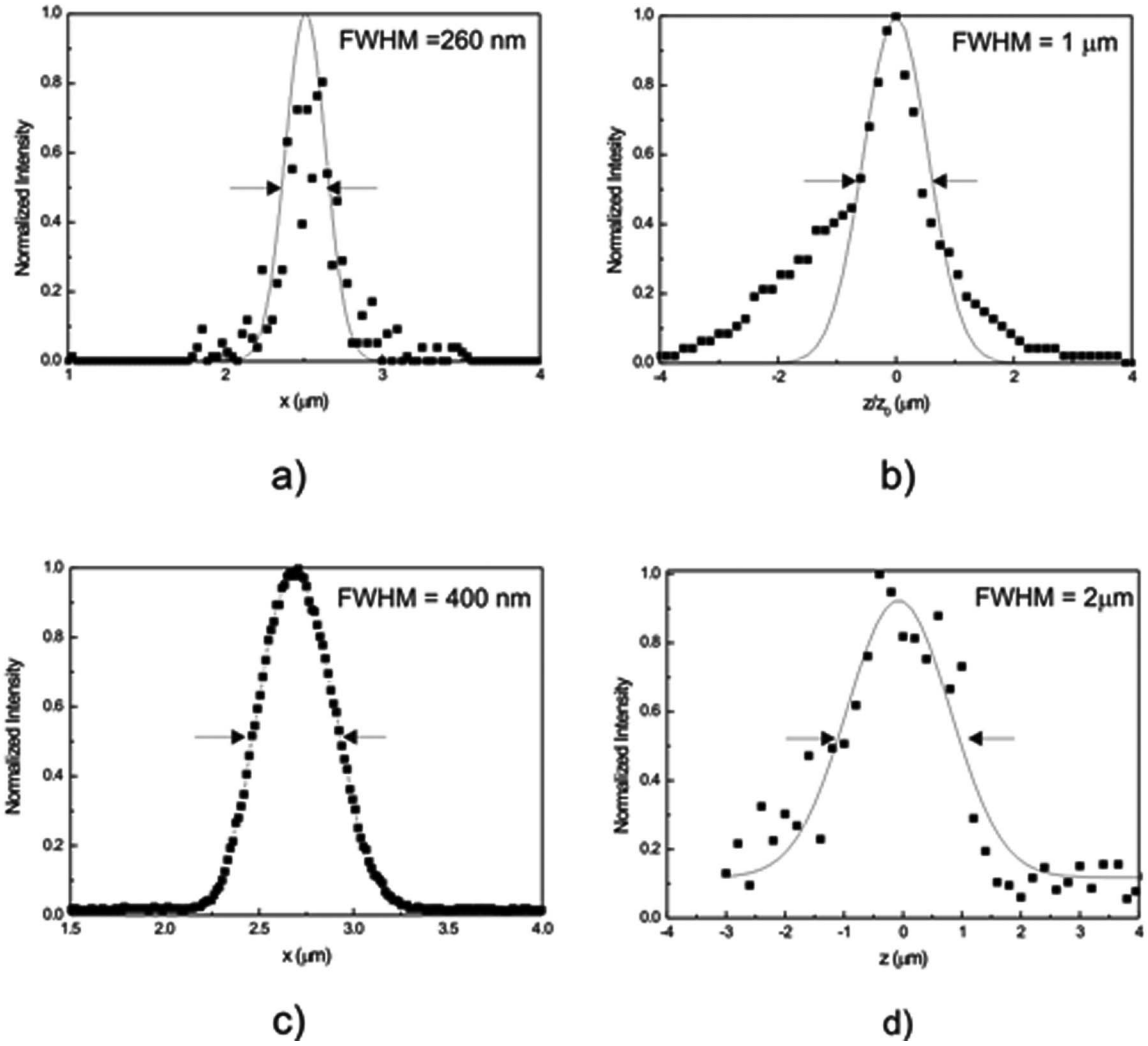

FIG. 3. Cross-sections of the measured PSFs (a) along the *x*- and *z*-axis (a and b, respectively) in the confocal mode and along the *x*- and *z*-axis in the TPF mode (c and d, respectively). The depicted curve is a Gaussian fitting to the obtained data. The diameters of the beads were 200 nm.

C. Simultaneous confocal, LSBF, and SHG microscopy

In simultaneous confocal, LSBF, and SHG microscopy both confocal and nonlinear microscopy subsystems work simultaneously. The filter cube FC2 in filter turret B is moved into the beam path to reflect the NIR femtosecond light (868 nm) onto the objective and the control software in PC2 is used to raster scan the femtosecond laser beam in a region of interest. The confocal SH delivers the excitation light through side port 1 which also collects the fluorescent emission light from confocal laser scanning. Here excitation light from the multiphoton system and confocal system interact simultaneously with the sample. Nevertheless, the presence of the confocal pinhole and the descanning rejects any light coming form outside the excitation volume of the confocal system (since there is no synchronization between the two scanning systems, they do not scan the same point at any instant of time). There is, hence, no interference created in the confocal images due to the laser scanning for nonlinear microscopy.

The filter cube FC3 is placed on top of the condenser to reflect the unconverted NIR light onto the PD and enable LSBF imaging. The optical fiber in the diascopic detector is inserted into the PMT module (P1) detecting the SHG signal. The narrow band pass filter in the PMT module blocks out most of the noise arising out of excitation or emission light, from the confocal laser scanning. This configuration enables simultaneous confocal, SHG/PSSHG, and LSBF imaging. The image acquisition in the confocal system is controlled by PC1 and that of LSBF and SHG controlled by PC2. Care has to be taken to use this configuration if any of the wavelengths chosen for confocal excitation or the fluorescent emission lie in the same spectral region as the SHG emission.

The Fig. 5 shows the head of an adult *C. elegans* worm imaged simultaneously using LSBF, confocal and SHG imaging modalities. (a) The LSBF image of the whole scanned region can be observed in gray scale, (b) GFP-labeled neuron (cell body and axon) can be observed in green in the confocal image, (c) and the pharynx muscles can be observed in cyan color in the SHG image. The figure also depicts a (d) superposition of all the three image channels. To produce the superposition, the LSBF and SHG images are simply added since they are produced from the same scanning process. The

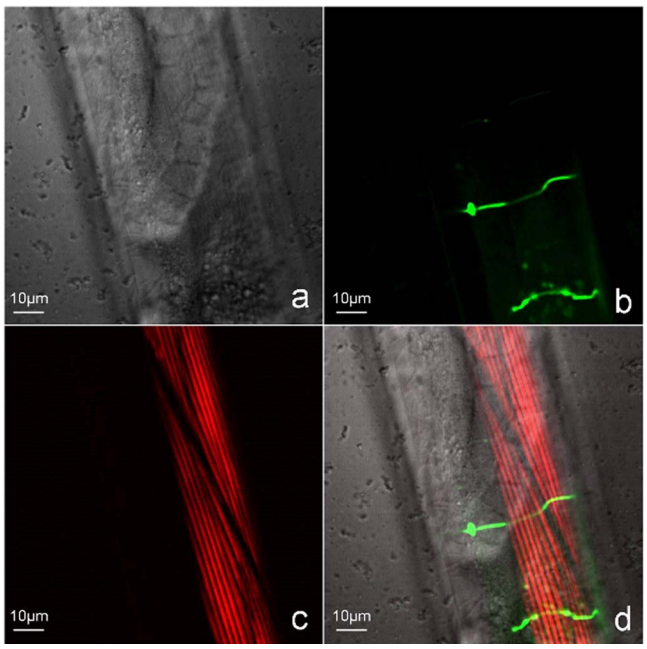

FIG. 4. (Color online) Simultaneous multimodal imaging of the midbody portion of adult *C. elegans* worm. (a) Brightfield (LSBF) image of the whole laser scanned area, (b) TPEF image of two *D*-type motor neurons expressing GFP (juIs76 [unc-25::gfp] II), (c) SHG image of body wall muscles, and (d) superposition of all the three image channels.

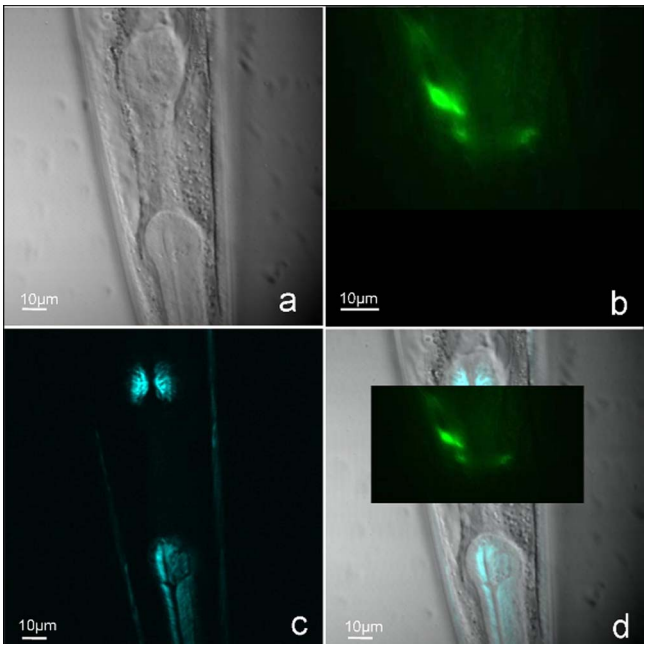

FIG. 6. (Color online) Simultaneous multimodal imaging of the head of an adult *C. elegans* worm (a) Brightfield (LSBF) image of the whole laser scanned area, (b) epifluorescence image of neurons expressing nmr-1::gfp, (c) SHG image of pharynx muscles, and (d) superposition of all the three images.

confocal image, having used a different scanner, had to be cut and resized separately for it to be superposed onto the combined LSBF and SHG images. The green fluorescence is produced from the GFP expressed in these neurons. An excitation laser wavelength of 488 nm is used to excite the GFP with the confocal system. As before, an excitation wavelength of 868 nm and imaging power of 15–18 mW on the sample plane are used for SHG and LSBF imaging.

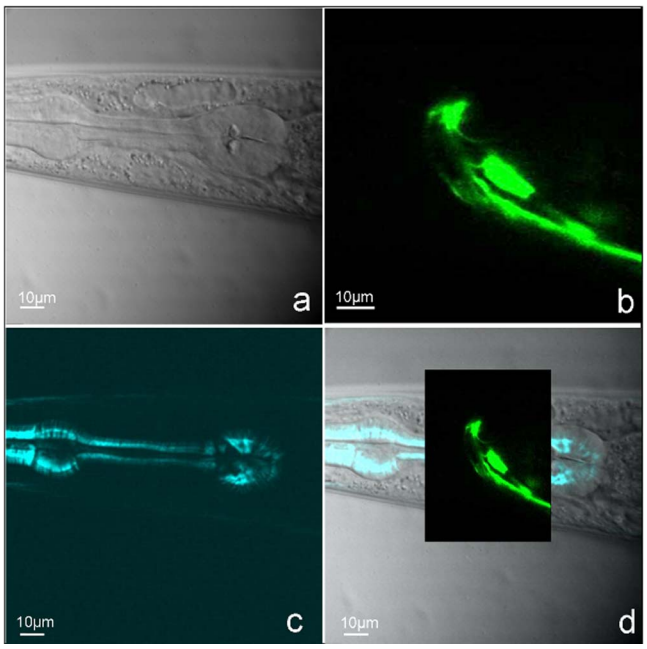

FIG. 5. (Color online) Simultaneous multimodal imaging of the head of an adult *C. elegans* worm. (a) Brightfield (LSBF) image of the whole laser scanned area, (b) confocal image of neurons expressing nmr-1::gfp, (c) SHG image of pharynx muscles, and (d) superposition of all the three images.

D. Simultaneous epifluorescence, LSBF, and SHG imaging

This mode is very similar to that presented in Sec. III, except that confocal imaging is replaced with epifluorescence imaging. In this mode FC2 and the appropriate filter cube FC1 in the filter turret A is inserted into the beam path. Subsequently the epifluorescence attachment is switched on and side port 3 with the CCD camera is connected, enabling acquisition of epifluorescence images in the CCD camera. Simultaneous SHG and brightfield imaging is performed, as described in Sec. I. The narrow band pass filter in the PMT module (P1) prevents most of the noise form the epifluorescence excitation/emission from interfering with the SHG imaging. Here again care has to be taken to use this configuration if any of the wavelengths chosen for epifluorescence excitation or the fluorescent emission lie in the same spectral region as the SHG emission.

Figure 6 shows the head of an adult *C. elegans* worm imaged simultaneously using LSBF, epifluorescence, and SHG imaging modalities. (a) LSBF image of the whole scanned region can be observed in gray scale, (b) GFP-labeled neurons can be observed in green in the epifluorescence image, (c) and the pharynx muscles can be observed in cyan color in the SHG image. The figure also depicts a (d) superposition of all the three image channels. The superposition was done as in the previous section. The green fluorescence is produced from the GFP expressed in these neurons. The fluorescein isothiocyanate (FITC) filter cube was used for epifluorescence imaging. As before, an excitation wavelength of 868 nm and imaging power of 15–18 mW on the sample plane were used for SHG and LSBF imaging.

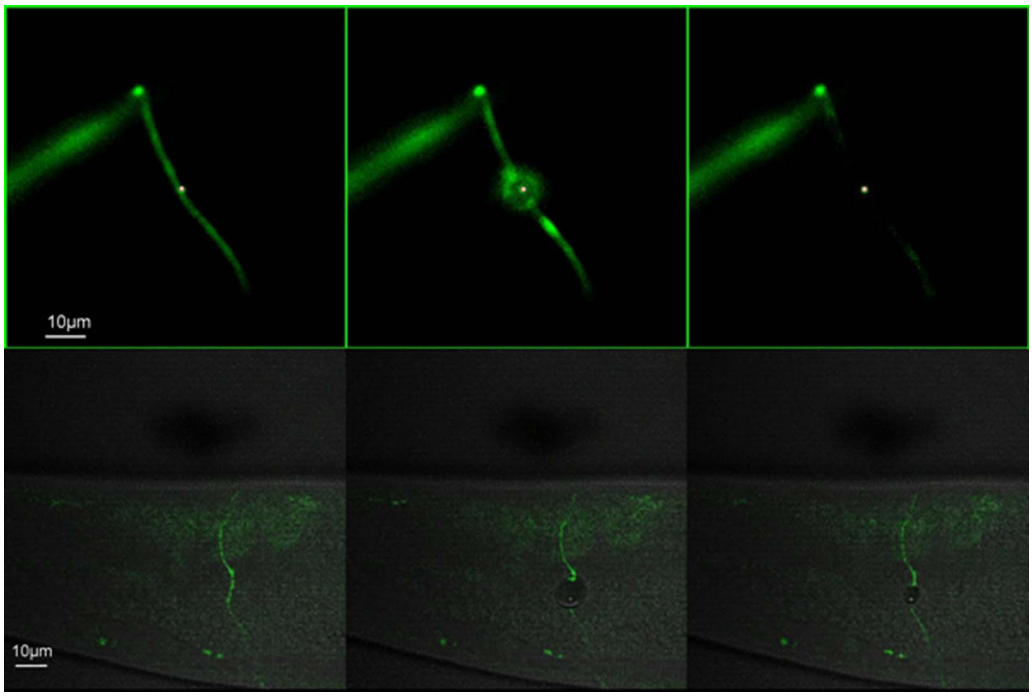

FIG. 7. (Color online) Time lapse images showing laser axotomy in an adult *C. elegans* worm imaged with both epi-fluorescence microscopy (A) and confocal microscopy (B). The green signal is form the GFP labeled neuron (unc-25::gfp). Red dot in A indicates the position of the laser beam (for details see Supplementary Movie-2).[26] In B the Brighfield image in gray scale is superposed with the confocal image (for details see Supplementary Movie-1).[26]

E. Simultaneous confocal, LSBF, and nanosurgery

A nonlinear microscope can readily be converted into a tool for nanosurgery. This is achieved by directing the femtosecond laser beam at very high intensity (above the damage threshold) using the scanning system to a specific point of interest. Ablation arises by the nonlinear absorption of laser light in the focal spot and can be well localized to the focal spot causing submicrometer incisions *in vivo* in biological samples without, or with significantly reduced, collateral damage.

The present system provides the possibility to use two independent laser-scanning systems and one of its strengths is its ability to perform real-time confocal imaging while the multiphoton part is let to perform the nanosurgery or, for that matter, any other photostimulation/photomanipulation. In this mode the filter cubes FC1 (in filter turret A) are moved out of the beam path, FC2 is inserted in, and the optical fiber in the diascopic system is inserted into the C1 control box enabling simultaneous confocal and brightfield imaging by PC1.

Side port 2 is initially connected and multiphoton microscopy is initiated. The control software in PC2 is used to select a target of interest for nanosurgery using a graphic user interface (GUI) based on the TPEF image. Multiphoton microscopy mode is subsequently terminated and side port 1 is connected to initiate confocal imaging using PC1, in a region of interest (which includes the region where the surgery would be performed). Afterwards, when the nanosurgery function in the LABVIEW program in PC2 is initiated, it closes the shutter. Once the shutter is closed, the program removes the attenuator 1 in the AS and inserts attenuator 2 (in order to let a preselected higher intensity of the laser beam pass for surgery). Subsequently the galvanometric mirrors are directed to the selected target and the shutter is opened for a specified time duration (usually few hundred milliseconds). The shutter is then closed and the attenuator 1 is placed back bringing down the optical power ready for imaging. The high laser power when let into the objective for a very short duration produces the submicrometer (usually close to diffraction limit) incision at the focal point. At the same time the confocal system generates confocal images and LSBF (using forward scattered confocal excitation light) images simultaneously. This enables high resolution and real-time observation of the surgical process and the events taking place in the neighborhood of the surgery.

Figure 7 shows a time lapse image of the nanoaxotomy procedure and the subsequent effects which were imaged using confocal microscopy (see lower panel of Fig. 7). The green signal is from the GFP-labeled motor neurons. The gray scale regions show the LSBF image generated by the confocal diascopic detection system, generated simultaneously with confocal microscopy. The impact of the femtosecond laser on the axon severs it. Meanwhile a cavitation bubble is formed that produces a rupture in the cuticle. The ruptured cuticle closes back and is almost unnoticeable after a short while.[26] This process would have gone unnoticed if the procedure of axotomy was not imaged in real time using simultaneous confocal and brightfield imaging. The axotomy was performed using a wavelength of 880 nm with an average power of about 90 mW (~1.2 nj/pulse at 76 MHz repetition rate) on the sample plane, by keeping the femtosecond beam static on the axon for about 100 ms using the electronic shutter. The confocal system was used to image the GFP tagged neuron using 488 nm excitation along with brightfield imaging using the diascopic system of the confocal microscope.

F. Simultaneous epifluorescence imaging and nanosurgery

In simultaneous epifluorescence imaging and nanosurgery the configuration is very similar to the ones used in previously published works.[27,28] Both FC2 and the appropriate filter cube FC1 (in the filter turret A) are moved into the beam path, the EP is switched on and the backward fluorescence emission is directed into side port 3 with the CCD camera enabling acquisition of epifluorescence images.

The control program selects a target using a GUI based on the CCD image. Nanosurgery is performed, as described in Sec. III using the nanosurgery function in the LABVIEW program in PC2, while the CCD camera captures the process in real time, in the form of fluorescence images.

Figure 7 shows time lapse images of the nanoaxotomy procedure and the subsequent effects that take place in the vicinity of the point of surgery imaged using epifluorescence microscopy (see upper panel of Fig. 7). The impact of the laser severs the axon and also creates a damage in the surrounding muscle. The impact of the laser also results in muscular elongation. The whole worm body can be seen stretching and relaxing back in a short while.[26] This process, again, can only be visualized through simultaneous imaging along with the axotomy.

G. Brightfield imaging

Brightfield images in this workstation can be generated in three ways: (a) by a CCD camera with bright light illumination; (b) using LSBF modality by scanning the femtosecond NIR light (using forward scattered femtosecond NIR excitation light) in the multiphoton mode, and; (c) by using LSBF in the confocal mode (detecting forward scatter confocal excitation light) using the diascopic detector. The LSBF modality generates high degree of image detail, which is comparable to a great extent to the DIC microscopy image (results not presented).

H. SHG and PSSHG imaging

SHG imaging, as already mentioned before, can be obtained either with a 0.5 or 1.4 NA condenser front lens. Ideally excitation with a high NA objective would need a high NA condenser for the collection of the emitted SHG signal. However, even with the use of the most commonly used 0.5 NA condenser that comes prefitted in most confocal microscopes, quite a high degree of image detail can be obtained. Replacing the 0.5 NA condenser with a 1.4 NA condenser improved the signal to noise ratio by 30% (image analysis in IMAGEJ; data not shown).

A polarizer and a HP placed outside the microscope provide an extra imaging technique: PSSHG imaging. SHG microscopy can provide structural information below the resolution limit of excitation light. This is because of the coherent nature of parametric nonlinear processes and dependence of these processes on the structural organization of the interacting medium. PSSHG imaging has been especially used for this purpose. PSSHG generation is also a capability of our multimodal workstation and can be achieved by rotating the HP in fixed increments (results not presented).

V. DISCUSSION

By using a commercially available confocal microscope as a base we have demonstrated how it can be adapted to form a multimodal workstation that comprises linear and multiphoton microscopic abilities. The system offers the ability for both systems to work simultaneously hence converting the confocal microscope into a multimodal workstation. This is achieved by using "off the shelf" components that can be readily inserted, attached, or appended externally to the confocal microscope, making the whole system very flexible to the user's needs.

In this workstation we have been able to combine confocal microscopy, epifluorescence microscopy, LSBF imaging, TPEF microscopy, SHG (and PSSHG) microscopy, and nanosurgery. In addition to nanosurgery[9,10,29] a nonlinear microscope could be readily adapted as a tool for other nanomanipulation techniques, such as multiphoton stimulation,[30] multiphoton uncaging of caged neurotransmitters,[31] optical knock out of cell organelles,[32] and intracellular chromosome dissection.[33] The setup we propose provides the possibility of combining all these techniques with real-time confocal or epifluorescene imaging. The laser-scanning system in the multiphoton component can also be used to induce linear effects such as optical tweezing,[34,35] photoporation[36] and Raman imaging,[37] which could also be combined with simultaneous confocal or epifluorescence imaging. In general, the advantage of having two independent laser-scanning imaging sets onto one microscope is that while one set is inducing an optical effect (such as optical tweezing, nanosurgery, or photostimulation) the other set can be imaging this procedure simultaneously in real time. A practical example is presented in this work where while the multiphoton set is performing nanosurgery, the confocal part is imaging this process in real time. This provides a way to reveal many events that happens along with the nanosurgery procedure. The illustrative examples for nanoneurosurgery in this paper were specially selected to reveal effects such as muscle and cuticle damage, that sometimes happen along with the process of nanosurgery, but go unnoticed due to the lack of simultaneous imaging functionality.

Such microscopy systems, where simultaneous imaging and optical stimulation is possible, do exist commercially.[17,18] The presently available commercial system has both the imaging and stimulation part both based on using nonlinear excitation. This is quite distinct from the work here presented where we combine linear and nonlinear imaging techniques that can be used simultaneously, in addition to the multiple applications for photomanipulation/stimulation (linearly or nonlinearly). Moreover, the work here presented emphasizes our efforts for upgrading, in a cheap and natural way, a fully automated commercial confocal microscope without compromising any of its functions.

Most laboratories have confocal microscopes as a central facility and the possibility to mechanically/electronically modify the confocal microscope into a multiphoton microscope is seldom possible. This work demonstrates the possibility of a conversion without the need for any irreversible

modifications. The normal functionality of the confocal microscope in this workstation is, in no way, affected. The components added directly onto the microscope are standard off the shelf attachments available from the microscope manufacturer. The rest of the components are placed external to the microscope. This allows to readily return the microscope back to its original "*status quo*." In addition, the excitation laser beam of the nonlinear system is brought in from an adjacent room into the confocal facility. This provides a solution to a frequently encountered situation in which there is little possibility of placing systems (such as femtosecond lasers) and subsystems in the same facility as the confocal microscope station. The fact that each system (both the linear and the nonlinear system) has the characteristics of a dedicated system is also a great asset of this workstation. In principle, provided that there are available ports with sufficient transmission and there is a prospect for having two filter turrets (or simply a possibility to include an extra dichroic mirror and enough space for the entrance of an external laser beam), there is a clear prospect for similar upgrades to other confocal microscopes.

Brightfield images generated by the conventional microscopy methods are usually achieved by a CCD camera with bright light illumination. In multiphoton microscopy the capture of these images needs to be done before or after the sample is imaged/manipulated. This presents two distinct drawbacks: (1) brightfield image cannot be generated simultaneously with multiphoton imaging and (2) there is no direct correspondence between the two image sets (brightfield and multiphoton) in terms of pixel resolution and imaged area. Brightfield imaging using forward scattered excitation light, as presented in this work, obviates these drawbacks allowing simultaneous brightfield imaging and multiphoton imaging. Since both the image sets (LSBF and multiphoton) are generated from the same scanning process, there is a direct one to one correspondence between the brightfield image and SHG/TPEF images and a perfect superposition of these two/three imaging modalities is obtained. This helps a great deal in precisely locating the origin of SHG/TPEF in the biological specimen. Moreover in time lapse imaging of dynamic processes it is very helpful to have a brightfield image for every corresponding TPEF\SHG image so that these dynamic processes could be precisely mapped onto the body of the biosample.

The present C1-Si confocal system features simultaneous excitation with seven different wavelengths and detection in either three channel or spectrally resolved modes. Simultaneous excitation with multiple wavelengths for TPEF would require a number of femtosecond lasers working at different wavelengths. This is, obviously, cost and space prohibitive. Accordingly, when it comes to multispectral excitation and detection the confocal microscope still holds an edge when compared to TPEF microscopy. The described workstation provides the user with the flexibility of combining SHG and brightfield imaging with either confocal imaging or TPEF imaging (depending on whether advantages of TPEF or confocal imaging are required).

In order to achieve SHG microscopy, a forward collecting mount is normally required, since the harmonic generation signal preferentially travels in the forward direction. In setups used by most research groups for this purpose, forward mounts, specially fabricated for the purpose, are used. In this work the standard 0.5 NA DIC condenser, in conjunction with the diascopic detector (which forms part of the confocal microscope), were directly used to collect the forward scattered SHG signal without any overhead. To collect in the full NA while excitation with high NA objectives a 1.4 NA oil immersion condenser replaces the 0.5 NA condenser providing very high quality SHG images. A polarizer and a HP placed outside the microscope provide an extra imaging technique: PSSHG imaging that can provide structural information below the resolution limit of excited light.

Nonlinear microscopes are increasingly being used not only for nonlinear imaging but also, after some minor changes, for cell/tissue/substrate manipulation techniques. A common drawback when performing techniques such as nanosurgery is that imaging cannot be performed simultaneously with the nanosurgery. Real-time imaging is essential to capture the surgery progression as well as events taking place immediately after the surgery in and around the region where surgery was performed. A number of works have used the epifluorescence microscopy in conjunction with nanosurgery for real-time imaging of the surgical procedure.[27,28] Epifluorescence microscopy, however, does not provide the axial resolution or clarity of nonlinear microscopy or confocal microscopy. The setup described here provides real-time confocal microscopy along with nanosurgery.

Even though epifluorescence microscopy does not provide the sharpness in image quality or the depth resolution as in confocal microscopy, it might prove useful. Epifluorescence microscopy using a CCD camera is much faster than laser-scanning techniques. Moreover, combining epifluorescence microscopy with nanosurgery or SHG and brightfield imaging enables a number of features of this workstation when built on a standard microscope (without the confocal imaging attachment). This could be, in many situations, an economical alternative to a confocal system.

VI. CONCLUSIONS AND PROSPECTS

Although the presented results in this work demonstrate only a small subset of the capabilities of the system, numerous other applications exist in which combined linear and nonlinear optical techniques, or induction of an optical effect with one system while imaging with the other, are required and aimed for. All such applications could make use of this workstation. In this manuscript we present some practical applications of the developed workstation in the field of cell biology. Nevertheless, there is a vast field of possible applications that could benefit with the use of this tool.

The presented system has great potential and large room for prospective improvements. THG can replace SHG if longer wavelengths for excitation are used. It is also possible to image THG and SHG simultaneously by adding another dichoric mirror in a fourth filter cube (FC4) that could be placed above the filter cube FC3 (positioned on top of the condenser). If a dichroic is so selected, so as to reflect the THG, it could be detected by a detector placed outside the

microscope while the SHG could be allowed to propagate into the optical fiber in the diascopic detector.

Presently the software that operate the confocal and the multiphoton systems are independent and running in different computers. In the near future the software can be brought together into one single platform. This would provide better synchrony and coherence among the two systems, especially when it comes to defining a common region of interest, time lapse imaging, etc.

The nonlinear component of the system can also be used to induce linear effects, such as optical tweezing, merely by switching the laser mode to CW. For example, while the second system performs optical tweezing, the confocal or epifluorescence component could be imaging the process in real time.

In summary, the multimodal workstation described here offers a highly flexible, versatile, and complete solution, providing an extremely useful tool of investigation in biology simultaneously using a combination of linear and nonlinear techniques. This upgrade can be incorporated in any commercial confocal microscope provided that there are available ports and there is a prospect for having two filter turrets (or possibility to include an extra dichroic mirror and enough space for the entrance of an external laser beam).

ACKNOWLEDGMENTS

The authors thank funding from Generalitat de Catalunya and the Ministerio de Educación y Ciencia (Grant Nos. CIDEM-RDITSCON07-1-0006 and TEC2006-12654), Grupo Ferrer and the European Regional Development Fund. We thank César Alonso Ortega for strain maintenance and sample preparation, Iain G. Cormack for design of the image acquisition module in the LABVIEW program and invaluable comments, Giovanni Volpe for invaluable comments and Tania Gomez for multimedia design. Moreover, we would like to thank Dr. Joe Culotti, from the Samuel Lunenfeld Research Institute (Toronto) who provided us with one of the worm strains. Some nematode strains used in this work were provided by the Caenorhabditis Genetics Center, which is funded by the NIH National Center for Research Resources (NCRR). We also thank the support given by Izasa S.A and Nikon Inc. This research has been partially supported by Fundació Cellex. Manoj Mathew and Susana I. C. O. Santos contributed equally to this work.

[1] P. Benedetti, Eur. J. Histochem. **42**, 11 (1998).
[2] T. Wilson, *Confocal Microscopy* (Academic, London, 1990).
[3] M. Terasaki and M. E. Dailey, in *Handbook of Biological Confocal Microscopy*, edited by J. B. Pawley (Plenum, New York, 1995), pp. 327–346.
[4] W. Denk, J. H. Strickler, and W. W. Webb, Science **248**, 73 (1990).
[5] P. J. Campagnola and L. M. Loew, Nat. Biotechnol. **21**, 1356 (2003).
[6] A. Squier, M. Muller, G. J. Brakenhoff, and K. R. Wilson, Opt. Express **3**, 315 (1998).
[7] D. Yelin and Y. Silberberg, Opt. Express **8**, 169 (1999).
[8] P. Stoller, K. M. Reiser, P. M. Celliers, and A. M. Rubenchik, Biophys. J. **82**, 3330 (2002).
[9] B. G. Wang, I. Riemann, H. Schubert, D. Schweitzer, K. Konig, and K. J. Halbhuber, Lasers Surg. Med. **39**, 527 (2007).
[10] A. K. N. Thayil, I. G. Cormack, A. Pereira, E. M. Blanco, M. Mathew, D. Artigas, and P. Loza-Alvarez, J. Microsc. **232**, 362 (2008).
[11] For further details on the Nikon confocal microscope please check http://www.nikoninstruments.com/c1si/.
[12] A. Ridsdale, I. Micu, and P. K. Stys, Appl. Opt. **43**, 1669 (2004).
[13] K. König, U. Simon, and K. J. Halbhuber, Cell. Mol. Biol. (Paris) **42**, 1181 (1996).
[14] A. Diaspro, M. Corosu, P. Ramoino, and M. Robello, Microsc. Res. Tech. **47**, 196 (1999).
[15] A. Majewska, G. Yiu, and R. Yuste, Eur. J. Phys. **441**, 398 (2000).
[16] V. Nikolenko, B. Nemet, and R. Yuste, Methods **30**, 3 (2003).
[17] http://www.olympusamerica.com/seg_section/product.asp?product=1020.
[18] http://www.zeiss.com/c12567be0045acf1/Contents-Frame/86b9882199315975c125709f003e8f07.
[19] M. Goksör, J. Enger, and D. Hanstorp, Appl. Opt. **43**, 4831 (2004).
[20] T. B. Huff, Y. Shi, Y. Fu, H. Wang, and J. X. Cheng, IEEE J. Sel. Top. Quantum Electron. **14**, 4 (2008).
[21] S. Tsai, N. Nishimura, E. J. Yoder, A. White, E. Dolnick, and D. Kleinfeld, in *Methods for In Vivo Optical Imaging* (CRC, Boca Raton, FL, 2002), pp. 113–171.
[22] http://www.nikoninstruments.com/ti/.
[23] S. Brenner, Genetics **77**, 71 (1974).
[24] H. Yoo, I. Song, and D. G. Gweon, J. Microsc. **221**, 172 (2006).
[25] A. W. Bigelow, C. R. Geard, G. Randers-Pehrson, and D. J. Brenner, Rev. Sci. Instrum. **79**, 123707 (2008).
[26] See EPAPS Document No. E-RSINAK-80-003906 for Movie-1 where simultaneous imaging of the nanoaxotomy allows visualization of immediate effects and for Movie-2 where simultaneous imaging of the nanoaxotomy with epifluorescence allows visualization of immediate effects. For more information on EPAPS, see http://www.aip.org/pubservs/epaps.html.
[27] M. F. Yanik, H. Cinar, H. N. Cinar, A. D. Chisholm, Y. Jin, and A. Ben-Yakar, Nature (London) **432**, 822 (2004).
[28] S. H. Chung, D. A. Clark, C. V. Gabel, E. Mazur, and A. D. T. Samuel, BMC Neurosci. **7**, 30 (2006).
[29] A. Vogel, J. Noack, G. Hüttman, and G. Paltauf, Appl. Phys. B: Lasers Opt. **81**, 1015 (2005).
[30] H. Hirase, V. Nikolenko, J. H. Goldberg, and R. Yuste, J. Neurobiol. **51**, 237 (2002).
[31] E. M. Callaway and R. Yuste, Curr. Opin. Neurobiol. **12**, 587 (2002).
[32] L. Sacconi, I. M. Tolic-Nørrelykke, M. D'Amico, F. Vanzi, M. Olivotto, R. Antolini, and F. S. Pavone, Cell Biochem. Biophys. **45**, 289 (2006).
[33] K. König, I. Riemann, and W. Fritzsche, Opt. Lett. **26**, 819 (2001).
[34] G. Volpe, G. P. Singh, and D. Petrov, Appl. Phys. Lett. **88**, 231106 (2006).
[35] G. Volpe, G. Volpe, and D. Petrov, Phys. Rev. E **76**, 061118 (2007).
[36] L. Paterson, B. Agate, M. Comrie, R. Ferguson, T. K. Lake, J. E. Morris, A. E. Carruthers, C. T. A. Brown, W. Sibbett, P. E. Bryant, F. Gunn-Moore, A. C. Riches, and K. Dholakia, Opt. Express **13**, 595 (2005).
[37] C. M. Creely, G. Volpe, G. P. Singh, M. Soler, and D. V. Petrov, Opt. Express **13**, 6105 (2005).